ACTA ABP BIOCHIMICA POLONICA

Vol. 70, No 1/2023
31–36
https://doi.org/10.18388/abp.2020_5971

Regular paper

Overexpressed *RAD51* promoted osteogenic differentiation by activating IGF1R/PI3K/AKT pathway in osteoblasts

Minli Qiu, Ya Xie, Liudan Tu, Minjing Zhao, Mingcan Yang, Linkai Fang and Jieruo Gu✉

Department of Rheumatology, The Third Affiliated Hospital of Sun Yat-Sen University, 600 Tianhe Road, Tianhe District, Guangzhou, 510630, China

Background: Osteoporosis (OP) is a skeleton disease induced by imbalance between osteoblast and osteoclast. Osteogenic differentiation of osteoblasts is of great importance, and the regulatory mechanisms are urgent to be studied. Methods: Differentially expressed genes were screened from microarray profile related to OP patients. The dexamethasone (Dex) was used to induce osteogenic differentiation of MC3T3-E1 cells. MC3T3-E1 cells were exposed to microgravity environment to mimic OP model cells. Alizarin Red staining and alkaline phosphatase (ALP) staining were used to evaluate the role of *RAD51* in osteogenic differentiation of OP model cells. Furthermore, qRT-PCR and western blot were applied to determine expression levels of genes and proteins. Results: *RAD51* expression was suppressed in OP patients and model cells. Alizarin Red staining and ALP staining intensity, the expression of osteogenesis-related proteins including runt-related transcription factor 2 (Runx2), osteocalcin (OCN), and collagen type I alpha1 (COL1A1) were increased by over-expressed *RAD51*. Furthermore, *RAD51* related genes were enriched in IGF1 pathway, and up-regulated *RAD51* activated IGF1 pathway. The effects of oe-RAD51 on osteogenic differentiation and IGF1 pathway were attenuated by IGF1R inhibitor BMS754807. Conclusions: Overexpressed *RAD51* promoted osteogenic differentiation by activating IGF1R/PI3K/AKT signaling pathway in OP. *RAD51* could be a potential therapeutic marker for OP.

Keyword: osteoporosis, osteogenic differentiation, *RAD51*, IGF1R/PI3K/AKT

Received: 21 October, 2021; revised: 11 January, 2022; accepted: 21 March, 2022; available on-line: 16 January, 2023

✉e-mail: gujieruo@163.com
Acknowledgements of Financial Support: This study was supported by National Natural Science Foundation of China, No.82071587.
Abbreviations: BMD, bone mineral density; OP, Osteoporosis;

INTRODUCTION

Osteoporosis (OP) has become one of the epidemic diseases affecting people's quality of life due to its diverse etiology and complex molecular mechanism. OP is characterized by decreased bone mass, destroyed microstructure of bone tissue, increased bone brittleness, as well as high rate of fracture(Lupsa & Insogna, 2015).

Currently, bone mineral density (BMD) is the accepted gold standard for the diagnosis of OP, but due to its low sensitivity, many patients with potential fracture risk will be missed (Lupsa & Insogna, 2015; Black & Rosen, 2016). At present, systemic drug therapy is the main treatment for OP. However, the emerging side effects neutralized the clinical outcome. For instance, bisphosphonates may lead to mandibular osteonecrosis; hormones are associated with an increased risk of cardiovascular disease; the composition of traditional Chinese medicine is complex and its efficacy is not exact. Therefore, it is of great significance to find safer and more effective treatments (Miller, 2016; Liu *et al.*, 2018).

The basic process of bone formation is divided into bone formation and bone resorption, which are reflected as the dynamic balance between osteoblasts and osteoclasts at the cellular level (Chen *et al.*, 2018; Li *et al.*, 2019). The processes of osteogenic and osteoclastic differentiation are influenced by a variety of cytokines, cellular signaling pathways, and intercellular communication (Muruganandan *et al.*, 2020; Yang *et al.*, 2020). In recent years, the researches have attached great attention to on its complex molecular biological mechanism

Gene therapy, as a rising therapeutic method in recent years, can be targeted for gene defects and diseased tissues of diseases, direct to the lesions, with little side effects (Shan *et al.*, 2019; Fei *et al.*, 2020; Gu *et al.*, 2020; Bonnet *et al.*, 2019). The human *RAD51* gene located at 15q15.1 has been found to be aberrant expressed in OP through microarray analyses. The RAD51 protein interacts with the ssDNA-binding protein replication protein A (RPA) and RAD52, and is involved in DNA homologous pairing and chain transfer (Bonilla *et al.*, 2020; Wassing & Esashi, 2021). Studies have shown that *RAD51* is abnormally expressed in breast cancer (Cruz *et al.*, 2018), cervical cancer (Sun *et al.*, 2020), pancreatic cancer (Zhang *et al.*, 2019), prostate cancer (Maranto *et al.*, 2018), esophageal cancer (Wang *et al.*, 2019), and is associated with poor prognosis (Zhang *et al.*, 2019; Zhang *et al.*, 2019; Xue, *et al.*, 2019). What's more, bone marrow mesenchymal stem cell (BMMSC)-derived exosomes restore radiation-induced bone loss by alleviating DNA and oxidative stress damage (Zuo *et al.*, 2019). Hence, we suspected that *RAD51* may be a novel target for OP.

Thereby, this study aimed to elucidate the regulatory mechanisms of *RAD51* in osteogenic differentiation. These findings may help to uncover newfound diagnostic biomarkers for OP.

MATERIALS AND METHODS

Bioinformatics

A microarray profile GSE100609 associated with genes of Indian post menopausal female and non-OP post menopausal female was downloaded from the Gene Expression Omnibus (GEO) database (http://www.

ncbi.nlm.nih.gov/geo). R language was used to analyse the dataset, then limma package was applied to identify all differentially expressed genes (DGEs) of OP group (n=4) and non-osteoporotic group (n=4). Finally DGEs in this study were screened under the standard of $P<0.05$ and $|\log_2 FC|\geq 1.5$, and the heatmap was drawn by heatmap package. Pearson correlation and KEGG analysis were also carried out to analyse DGEs.

Subjects

Total number of 80 volunteers (healthy controls, n=40; OP patients, n=40) in this study were from The Third Affiliated Hospital of Sun Yat-Sen University. All the volunteers have signed the informed consent. This study was approved by Ethics Committee of The Third Affiliated Hospital of Sun Yat-Sen University. Fasting blood was collected for the follow-up experimental studies.

Isolation of human monocytes

Peripheral blood samples were collected from patients with osteoporotic fractures in the case group and healthy controls, and monocytes were obtained by density gradient centrifugation using sodium citrate anticoagulation tube (Histopaque-1077; Sigma, New Jersey, USA). Then monocytes were incubated at 37°C under 5% CO_2 in a humidified atmosphere with DMEM (pH 7.2).

Cell culture

Osteoblastic MC3T3-E1 cells were purchased from the Cell Bank of the Chinese Academy of Sciences (Shanghai, China). MC3T3-E1 cells were incubated in α-MEM medium (Gibco, Grand Island, USA) containing 10% fetal bovine serum (FBS, Gibco, Grand Island, USA) in 5% CO_2 at 37°C.

OP model cell establishment

2D Rotating Wall Vessel Bioreactor (RWVB) clinostat was used to simulate microgravity. 1×10^5 of MC3T3-E1 cells were seededon cell climbing pieces. 1×10^5 MC3T3-E1 cells were seeded on coverslips. After culture for 24 h, the climbing pieces were placed in a box 12.5 mm away from therotational axis. After the air bubbles were removed, the chambers were fixed in the clinostat and rotated around a horizontal axis at 28 rpm for 15 min. The vertical rotation groups were used as controls. The rotation process was taken at 37°C under 5% CO_2.

Induction of osteogenic differentiation

Osteoblastic MC3T3-E1 cells were seeded into 6-well plates at a density of 5×10^4 cells per well, and cultured with 100 nM dexamethasone (Dex; Sigma, Merck, USA), 10 nM beta-glycerophosphate (Sigma, Merck, USA) along with 50 mg/mL ascorbic acid (Sigma, Merck, USA). The mixed medium were replenished every 3 days. Cells treated with Dex was deemed as negative control (NC), and microgravity stimulated cells treated with Dex were named as OP group.

Cell transfection

To detect the role of *RAD51* in osteogenic differentiation, over-expressed RAD51 (oe-RAD51) vector (GenePharma, Shanghai, China) was transfected into OP model cells using Lipofectamine3000 (Invitrogen, Carlsbad, USA) according to instruction manuals. The transfection efficiency was verified by qRT-PCR.

qRT-PCR

Total RNA was isolated from blood sample, monocytes, and MC3T3-E1 cells by Trizol method (Takara, Kyoto, Japan) and measured at the absorbance of 260 nm (NanoDrop 2000; Thermo Fisher, MA, USA). Then, quantified RNA were conversed into complementary DNA by the reverse transcription kit (TaKaRa, Kyoto, Japan) according to manufacturer's protocols. RT-PCR was then performed using Power SYBR® Green PCR Master Mix (Takara) on the ABI StepOnePlus System (Applied Biosystems, Warrington, UK). GAPDH was used as a housekeeping gene. The relative mRNA expressions were calculated using the $2^{-\Delta\Delta Ct}$ method. Primer sequences were listed in Table 1.

Table 1. Primer sequences

Primer	Sequence	
RAD51	forward	5′-TGGGTTTCACCACTGCAACT-3′
	reverse	5′-AAACATCGCTGCTCCATCCA-3′
Runx2	forward	5′-TAAGATGGGAGGGCGTGAGA-3′
	reverse	5′-GTCGAGAGGATGAAGGAGCG-3′
OCN	forward	5′-CACTCCTCGCCCTATTGGC-3′
	reverse	5′-CCCTCCTGCTTGGACACAAAG-3′
COL1A1	forward	5′-TGGATACTGGGAGGGTGAGG-3′
	reverse	5′-CCCTTACCTGAGATGGGGGA-3′
GAPDH	forward	5′-CGAGCCACATCGCTCAGACA-3′
	reverse	5′-GTGGTGAAGACGCCAGTGGA-3′

Alizarin red staining and alkaline phosphatase (ALP) staining

OP model cells were seeded into 12-well plates, and fixed with 4% paraformaldehyde (Sigma, New Jersey, USA) for 15 min, then washed with PBS for three times. For alizarin red staining, cells were washed with distilled water, and incubated with 0.5% solution of alizarin red solutions for 30 min at room temperature. Afterwards, the relative values of alizarin red staining were measured at 560 nm using a microplate reader (ELX808; BioTek). The readings of all samples were normalized to the alizarin red staining intensity. For ALP staining, an ALP Staining Kit (Beyotime, Nantong, China) was used after the cells were washed with distilled water for three times. The stained cells were photographed by a microscope (Zeiss, Oberkochen, Germany), and calculated at the absorbance of 562 nm using microplate reader (BioTek, Winooski, USA).

Western blot assay

OP model cells were lysed in a RIPA lysis buffer (Beyotime, Nantong, China) for 30 min at 4°C. The supernate was harvested by centrifuging at 12 000×*g* for 5 min at 4°C. The proteins were separated by 10% SDS-PAGE and transferred to polyvinylidene fluoride membranes (Millipore, MA, USA). Then the membranes were blocked with 5% skimmed milk for 1 h, and then incubated with primary antibodies, such as anti-Runx2 (1/1000, ab236639), anti-OCN (1/1000, ab133612), anti-COL1A1 (1/1000, ab34710), anti-IGF1R (1/1000, ab182408), and anti-p-IGF1R (1/1000, ab39398), anti-PI3K (1/1000, ab32089), anti-p-PI3K (1/1000, ab182651), anti-AKT (1/10000, ab179463),

anti-p-AKT (1/1000, ab38449), and GADPH (1/1000, ab8245) at 4°C overnight, and then with secondary antibody (1/5000, ab6721) for 1 h at room temperature. The Infrared Imaging System (LI-COR, Lincoln, USA) was used to scan and analyze the images. All antibodies were purchased from Abcam company (Cambridge, England).

Statistical analysis

Statistical analysis was performed with GraphPad Prism 8.3 (GraphPad, San Diego, USA). All data were expressed as mean ± S.D. Statistical comparisons were performed by using the student's t-test between two groups and one-way ANOVA followed by Tukey's test for multiple groups. *P* values less than 0.05 were considered as statistically significant.

RESULTS

RAD51 expression was decreased in OP

Firstly, we identified prominently expressed DEGs through the bioinformatic analysis, and the results showed that total number of 107 genes were abnormally down-regulated genes and 42 up-regulated, compared with healthy controls, among which *RAD51* expression was most significantly suppressed (Fig. 1A). To further verify the roles of *RAD51* in OP, we determined the expression of RAD51 in blood samples of OP patients. As shown in Fig. 1B, the mRNA expression of *RAD51* was significantly decreased in blood samples of OP patients compared with healthy controls (Fig. 1B). Furthermore, *RAD51* expression levels were also downregulated in isolated monocytes of patients with OP (Fig. 1C).

Osteogenic differentiation of OP model cells was weakened

Then, Dex was used to induce osteogenic differentiation of MC3T3-E1 cells, and osteogenic differentiation ability of OP model cells were measured. After microgravity stimulation, both alizarin red and ALP intensity of MC3T3-E1 cells were dramatically decreased, indicating that mineralization levels of OP model cells were declined (Fig. 2A–B). Meanwhile, both protein and mRNA expression levels of osteogenesis-related proteins including Runx2, OCN, and COL1A1 were markedly suppressed in OP model cells (Fig. 2C–E). Furthermore, *RAD51* was also suppressed in OP model cells (Fig. 2F). Hence, osteogenic differentiation of OP model cells was significantly weakened.

Up-regulated *RAD51* promoted osteogenic differentiation of OP model cells

Next, whether RAD51 could modulate osteogenic differentiation of MC3T3-E1 cells was investigated. After *RAD51* was prominently up-regulated in MC3T3-E1 cells transfected with overexpressed RAD51 vectors (Fig. 3A), alizarin red staining and ALP staining intensity of OP model cells were dramatically increased (Fig. 3B), so did the mRNA and protein expression levels of Runx2, OCN, and COL1A1 (Fig. 3C–D).

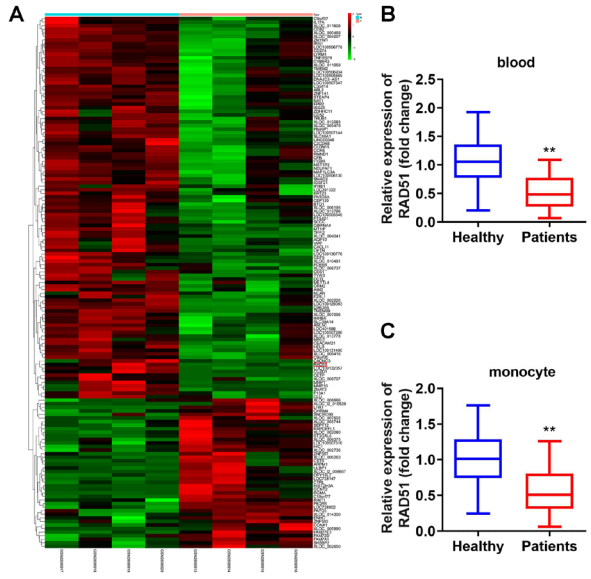

Figure 1. *RAD51* was suppressed in OP.
(**A**) heatmap consisting of post menopausal female and non-OP post menopausal female genes. The red represents the up-regulated genes and the green represents the down-regulated genes. *RAD51* expression detected by qRT-PCR of (**B**) blood and (**C**) monocytes of OP patients compared with healthy controls. ***P*<0.01. OP: osteoporosis.

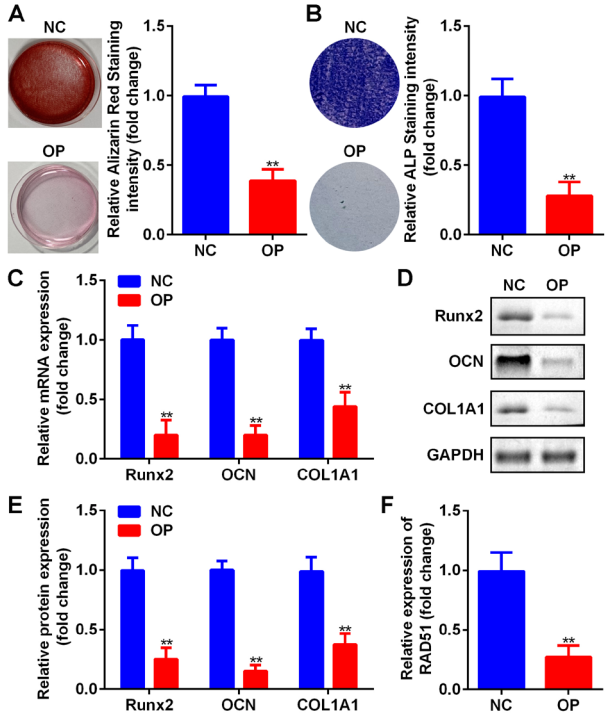

Figure 2. Osteoblast differentiation of OP model cells.
(**A**) Alizarin red staining images and intensity of MC3T3-E1 cells before and after microgravity stimulation. (**B**) ALP staining images and intensity of MC3T3-E1 cells before and after microgravity stimulation. (**C**) mRNA expression levels of Runx2, OCN, and COL1A1 in OP model cells measured by qRT-PCR. (**D**) Protein bands of Runx2, OCN, and COL1A1 in OP model cells measured by western blot. (**E**) Protein quantitative analysis of Runx2, OCN, and COL1A1. F. *RAD51* expression detected by qRT-PCR of OP model cells compared with control cells. ***P*<0.01.

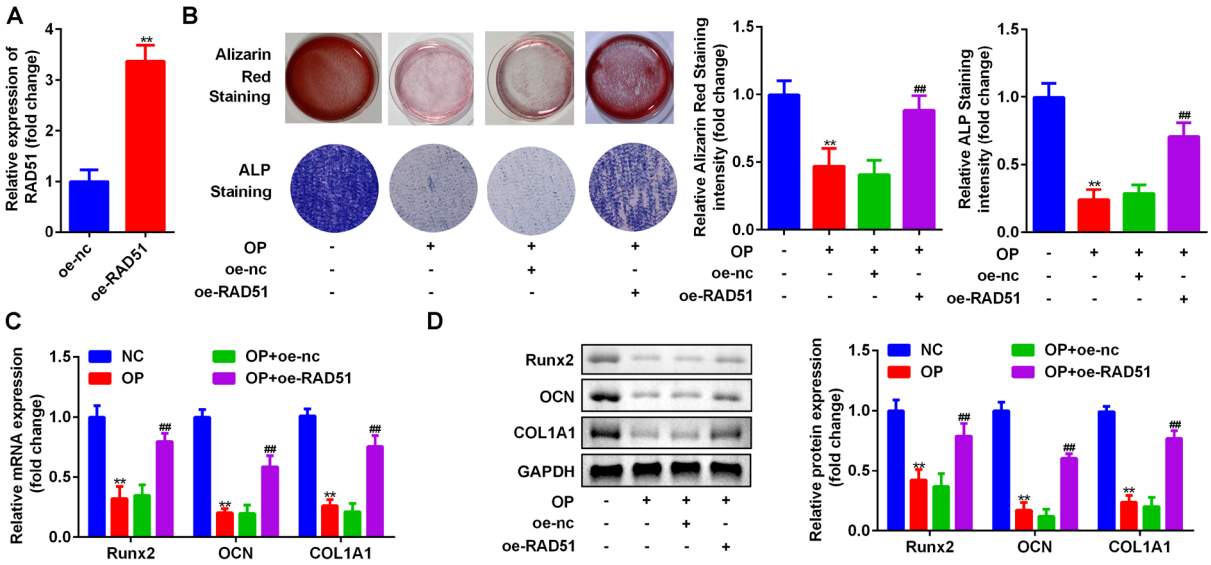

Figure 3. Up-regulated *RAD51* promoted osteogenic differentiation of OP model cells.
(**A**) Transfection efficiency of *RAD51* detected by qRT-PCR. B. Alizarin red staining and ALP images and intensity of OP model cells transfected with oe-RAD51 vectors. (**C–D**) Expression levels of Runx2, OCN, and COL1A1 measured by qRT-PCR and western blot of OP model cells. $^{**}P<0.01$, compared with oe-nc and NC group. $^{\#\#}P<0.01$, compared with OP+ oe-nc group. oe: overexpressed.

Over-expressed *RAD51* promoted osteogenic differentiation of OP model cells by activating IGF1R/PI3K/AKT signaling pathway

Subsequently, molecular mechanism of RAD51 regulating osteoporosis was then studied. Pearson correlation analysis between *RAD51* expression levels and other genes expression levels suggested that most aberrant expressed genes identified were positively related to *RAD51* (Fig. 4A). Subsequently, KEGG analysis demonstrated that genes related to *RAD51* were enriched in ten pathways, including IGF1 pathway, EGF receptor signaling pathway, C-MYB transcription factor network and so on. (Fig. 4B). Interestingly, downstream proteins in IGF1 pathway including phosphorylated IGF1R, PI3K, and AKT were up-regulated induced by oe-RAD51, suggesting the activation of IGF1R/PI3K/AKT signaling pathway (Fig. 5A). Meanwhile, alizarin red and ALP stained cells as well as expression of Runx2, OCN, and COL1A1 were markedly increased after *RAD51* was overexpressed in OP model cells (Fig. 5B–D). Furthermore, BMS754807, an IGF1R inhibitor, attenuated the effects of oe-RAD51 on mineral intensity and ALP activity number and the expression of Runx2, OCN, and COL1A1 (Fig. 5B–D).

DISCUSSION

OP has become one of the epidemic diseases affecting people's quality of life due to its diverse etiology and complex molecular mechanisms (Black & Rosen, 2016). In our study, *RAD51* was down-regulated in OP patients as well as OP model cells. Over-expressed *RAD51* promoted osteoblast differentiation by activating IGF1R/PI3K/AKT signaling pathway.

Recently evidence suggested that various aberrant expressed genes are involved in osteogenesis. For instance, osteogenic differentiation can be inhibited by blocking the correlation between RANKL and its only known receptor RANK (Bonnet *et al.*, 2019). Likewise, SOST secreted sclerostin to promote bone formation, thus alleviating the progression of OP (Shan *et al.*, 2019; Weivoda *et al.*, 2017). Our data suggested that *RAD51* was down-regulated in both OP patients and OP model cells.

Over the past decade, specific biochemical markers associated with metabolic bone disease have been identified and described to determine whether there is an imbalance in bone metabolism by measuring biochemical markers of bone turnover (Greenblatt *et al.*, 2017; Szulc, 2018). Our

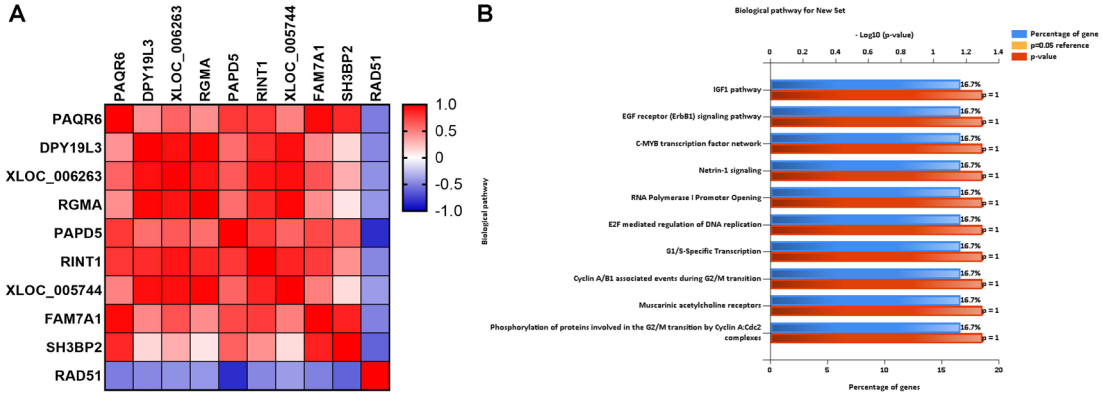

Figure 4. *RAD51* related genes were enriched in several pathways.
(**A**) Pearson correlation analysis between *RAD51* gene and other genes related with OP. (**B**) KEGG analysis of enriched genes associated with *RAD51* gene.

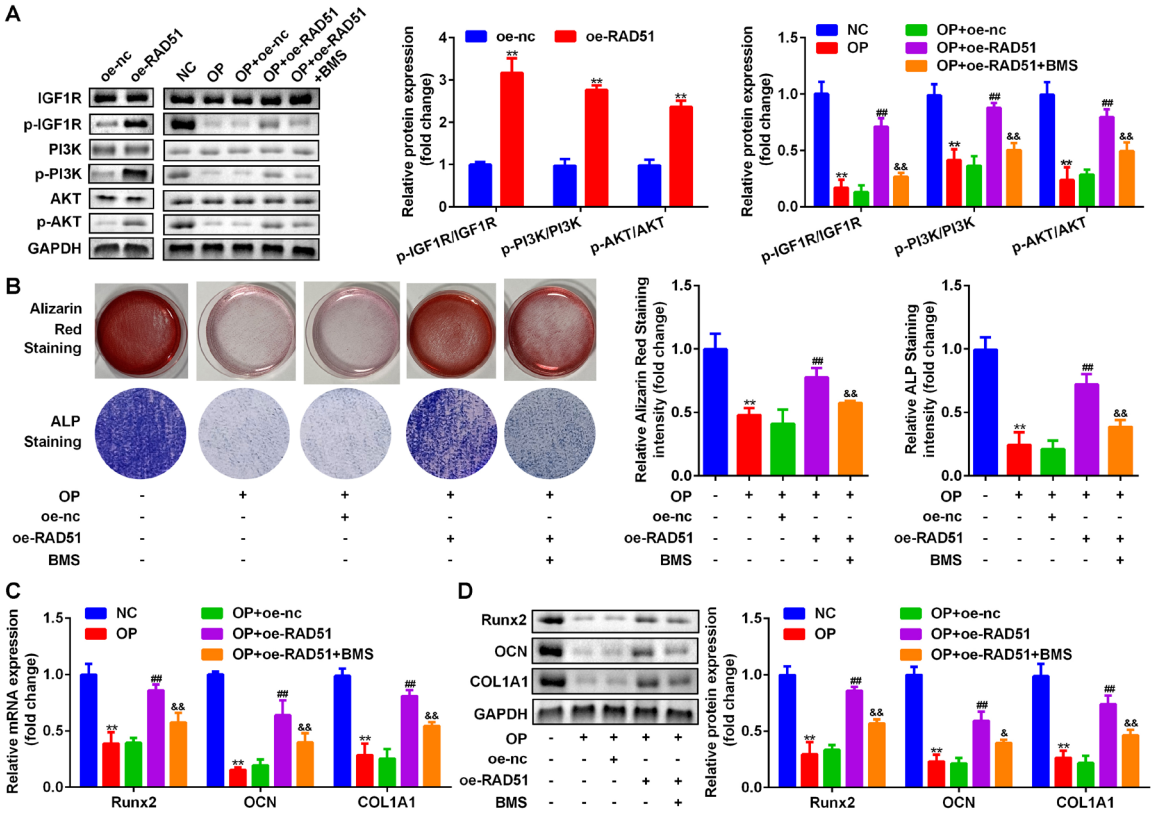

Figure 5. Over-expressed *RAD51* promoted osteogenic differentiation of OP model cells by activating IGF1R/PI3K/AKT signaling pathway.
(**A**) Protein expression of IGF1R, PI3K, AKT and their phosphorylated types measured by western blot assay. (**B**) Alizarin red staining and ALP staining images and intensity of OP model cells. (**C**) mRNA expression levels of Runx2, OCN, and COL1A1 measured by qRT-PCR. (**D**) Protein brands and quantitative analysis of Runx2, OCN, and COL1A1 measured by western blot. $^{**}P<0.01$, compared with oe-nc and NC group. $^{\#\#}P<0.01$, compared with OP+ oe-nc group. $^{\&}P<0.05$, $^{\&\&}P<0.01$, compared with OP+ oe-RAD51 group.

study showed that osteogenic differentiation was promoted as represented by higher Runx2, OCN and COL1A1 secretion. Runx2, OCN and COL1A1 were biochemical markers of OP widely studied in various studies. Runx2 is an osteoblast differentiation specific transcription factor which can regulate the transcription of many genes, and is significant for the differentiation of stromal cells into osteoblast lineage (Komori, 2018). Besides, Runx2 is reported to promote secretion of proteins including OPN, OCN, and collagen type I alpha1 (Yin *et al.*, 2019; Lu *et al.*, 2019; Komori, 2020). Furthermore, bone matrix mineralization is recognized as an indicator of osteogenic differentiation (Li *et al.*, 2018). In present study, the osteogenic differentiation, and the expression of *RAD51* of MC3T3-E1 cells was significantly suppressed by microgravity treatment. What's more, up-regulated *RAD51* promoted osteogenic differentiation of OP model cells, which was in line with previous studies (Shan *et al.*, 2019; Bonnet *et al.*, 2019; Weivoda *et al.*, 2017).

IGF-1 is known to play an anabolic role in bone (Frater *et al.*, 2018). Decreased IGF-1 levels are associated with an increased risk of bone fragility and fracture (Yan *et al.*, 2016). IGF1R is a homodimer of two protein subunits consisting of α and β chains, and is associated with bone and glucose metabolism and is a key mediator of glucose and bone metabolism disorders (Xian *et al.*, 2012). The conformation of IGF1R is altered by binding to the ligand IGF-1, which is then fully activated by ligand-independent autophosphorylation. This induces phosphorylation of various substrates, such as insulin receptor substrates and Shc proteins, and triggers specific signaling cascades, such as the PI3K/AKT and Ras/MAPK pathways (Yoshida & Delafontaine, 2020; Vitiello *et al.*, 2019).

In recent years, many studies have explored the influence of some factors on BMMSC through PI3K/AKT signaling pathway (Shen *et al.*, 2019). For instance, macrophage MSR1 contributed to osteogenic differentiation of BMMSC through PI3K/AKT pathway (Zhao *et al.*, 2020). Fang *et al* found that calycosin stimulates the osteogenic differentiation of rat calvarial osteoblasts by activating the IGF1R/PI3K/Akt signaling pathway (Fang *et al.*, 2019). Furthermore, our data demonstrated that the activation of IGF1R/PI3K/AKT signaling pathway induced by over-expressed *RAD51* was suppressed by IGF1R inhibitor, so did the osteogenic differentiation. These results indicated that up-regulated *RAD51* promoted osteogenic differentiation via activating IGF1R/PI3K/AKT signaling pathway.

CONCLUSION

In a word, overexpressed *RAD51* promoted osteogenic differentiation of osteoblasts via activating IGF1R/PI3K/AKT signaling pathway.

Declarations

Acknowledgments. Not Applicable.

Ethical approval. This study protocol was approved by the Ethics Committee of The Third Affiliated Hospital of Sun Yat-Sen University.

Informed consent. Informed onsent was obtained from all individual participants included in the study.

REFERENCES

Black DM, Rosen CJ (2016) Clinical Practice. Postmenopausal Osteoporosis. *N Engl J Med* **74**: 254–262. https://doi.org/10.1056/NEJMcp1513724

Bonilla B, Hengel SR, Grundy MK, Bernstein KA (2020) RAD51 gene family structure and function. *Annu Rev Genet* **54**: 25–46. https://doi.org/10.1146/annurev-genet-021920-092410

Bonnet N, Bourgoin L, Biver E, Douni E, Ferrari S (2019) RANKL inhibition improves muscle strength and insulin sensitivity and restores bone mass. *J Clin Invest* **129**: 3214–3223. https://doi.org/10.1172/JCI125915

Chen X, Wang Z, Duan N, Zhu G, Schwarz EM, Xie C (2018) Osteoblast-osteoclast interactions. *Connect Tissue Res* **59**: 99–107. https://doi.org/10.1080/03008207.2017.1290085

Cruz C, Castroviejo-Bermejo M, Gutiérrez-Enríquez S, Llop-Guevara A, Ibrahim YH, Gris-Oliver A, Bonache S, Morancho B, Bruna A, Rueda OM, Lai Z, Polanska UM, Jones GN, Kristel P, de Bustos L, Guzman M, Rodríguez O, Grueso J, Montalban G, Caratú G, Mancuso F, Fasani R, Jiménez J, Howat WJ, Dougherty B, Vivancos A, Nuciforo P, Serres-Créixams X, Rubio IT, Oaknin A, Cadogan E, Barrett JC, Caldas C, Baselga J, Saura C, Cortés J, Arribas J, Jonkers J, Díez O, O'Connor MJ, Balmaña J, Serra V (2018) RAD51 foci as a functional biomarker of homologous recombination repair and PARP inhibitor resistance in germline BRCA-mutated breast cancer. *Ann Oncol* **29**: 1203–1210. https://doi.org/10.1093/annonc/mdy099

Fang Y, Xue Z, Zhao L, Yang X, Yang Y, Zhou X, Feng S, Chen K (2019) Calycosin stimulates the osteogenic differentiation of rat calvarial osteoblasts by activating the IGF1R/PI3K/Akt signaling pathway. *Cell Biol Int* **43**: 323–332. https://doi.org/10.1002/cbin.11102

Fei Q, Li X, Lin J, Yu L, Yang Y (2020) Identification of aberrantly expressed long non-coding RNAs and nearby targeted genes in male osteoporosis. *Clin Interv Aging* **15**: 1779–1792. https://doi.org/10.2147/CIA.S271689

Frater J, Lie D, Bartlett P, McGrath JJ (2018) Insulin-like Growth Factor 1 (IGF-1) as a marker of cognitive decline in normal ageing: A review. *Ageing Res Rev* **42**: 14–27. https://doi.org/10.1016/j.arr.2017.12.002

Greenblatt MB, Tsai JN, Wein MN (2017) Bone turnover markers in the diagnosis and monitoring of metabolic bone disease. *Clin Chem* **63**: 464–474. https://doi.org/10.1373/clinchem.2016.259085

Gu Z, Xie D, Huang C, Ding R, Zhang R, Li Q, Lin C, Qiu Y (2020) MicroRNA-497 elevation or LRG1 knockdown promotes osteoblast proliferation and collagen synthesis in osteoporosis *via* TGF-beta1/Smads signalling pathway. *J Cell Mol Med* **24**: 12619–12632. https://doi.org/10.1111/jcmm.15826

Komori T (2020) Molecular mechanism of Runx2-dependent bone development. *Mol Cells* **43**: 168–175. 10.14348/molcells.2019.0244

Komori T (2018) Runx2, an inducer of osteoblast and chondrocyte differentiation. *Histochem Cell Biol* **149**: 313–23. https://doi.org/10.1007/s00418-018-1640-6

Li J, Li X, Liu D, Hamamura K, Wan Q, Na S, Yokota H, Zhang P (2019) eIF2alpha signaling regulates autophagy of osteoblasts and the development of osteoclasts in OVX mice. *Cell Death Dis* **10**: 921. https://doi.org/10.1038/s41419-019-2159-z

Li X, Zheng Y, Zheng Y, Huang Y, Zhang Y, Jia L, Li W (2018) Circular RNA CDR1as regulates osteoblastic differentiation of periodontal ligament stem cells *via* the miR-7/GDF5/SMAD and p38 MAPK signaling pathway. *Stem Cell Res Ther* **9**: 232. https://doi.org/10.1186/s13287-018-0976-0

Liu GF, Wang ZQ, Liu L, Zhang BT, Miao YY, Yu SN (2018) A network meta-analysis on the short-term efficacy and adverse events of different anti-osteoporosis drugs for the treatment of postmenopausal osteoporosis. *J Cell Biochem* **119**: 4469–4481. https://doi.org/10.1002/jcb.26550

Lu X, Lu J, Zhang L, Xu Y (2019) Effect of ANGPTL7 on proliferation and differentiation of MC3T3-E1 cells. *Med Sci Monit* **25**: 9524–9530. https://doi.org/10.12659/MSM.918333

Lupsa BC, Insogna K (2015) Bone health and osteoporosis. *Endocrinol Metab Clin North Am* **44**: 517–530. 10.1016/j.ecl.2015.05.002

Maranto C, Udhane V, Hoang DT, Gu L, Alexeev V, Malas K, Cardenas K, Brody JR, Rodeck U, Bergom C, Iczkowski KA, Jacobsohn K, See W, Schmitt SM, Nevalainen MT (2018) STAT5A/B Blockade sensitizes prostate cancer to radiation through inhibition of RAD51 and DNA repair. *Clin Cancer Res* **24**: 1917–1931. https://doi.org/10.1158/1078-0432.CCR-17-2768

Miller PD (2016) Management of severe osteoporosis. *Expert Opin Pharmacother* **17**: 473–488. https://doi.org/10.1517/14656566.2016.1124856

Muruganandan S, Ionescu AM, Sinal CJ (2020) At the crossroads of the adipocyte and osteoclast differentiation programs: future therapeutic perspectives. *Int J Mol Sci* **21**: 2277. https://doi.org/10.3390/ijms21072277

Shan Y, Wang L, Li G, Shen G, Zhang P, Xu Y (2019) Methylation of bone SOST impairs SP7, RUNX2, and ERalpha transactivation in patients with postmenopausal osteoporosis. *Biochem Cell Biol* **97**: 369–374. https://doi.org/10.1139/bcb-2018-0170

Shen WC, Lai YC, Li LH, Liao K, Lai HC, Kao SY, Wang J, Chuong CM, Hung SC (2019) Methylation and PTEN activation in dental pulp mesenchymal stem cells promotes osteogenesis and reduces oncogenesis. *Nat Commun* **10**: 2226. https://doi.org/10.1038/s41467-019-10197-x

Sun H, Fan G, Deng C, Wu L (2020) miR-4429 sensitized cervical cancer cells to irradiation by targeting RAD51. *J Cell Physiol* **235**: 185–193. https://doi.org/10.1002/jcp.28957

Szulc P (2018) Bone turnover: Biology and assessment tools. *Best Pract Res Clin Endocrinol Metab* **32**: 725–738. https://doi.org/10.1016/j.beem.2018.05.003

Vitiello PP, Cardone C, Martini G, Ciardiello D, Belli V, Matrone N, Barra G, Napolitano S, Della Corte C, Turano M, Furia M, Troiani T, Morgillo F, De Vita F, Ciardiello F, Martinelli E (2019) Receptor tyrosine kinase-dependent PI3K activation is an escape mechanism to vertical suppression of the EGFR/RAS/MAPK pathway in KRAS-mutated human colorectal cancer cell lines. *J Exp Clin Cancer Res* **38**: 41. https://doi.org/10.1186/s13046-019-1035-0

Wang J, Che W, Wang W, Su G, Zhen T, Jiang Z (2019) CDKN3 promotes tumor progression and confers cisplatin resistance *via* RAD51 in esophageal cancer. *Cancer Manag Res* **11**: 3253–3264. https://doi.org/10.2147/CMAR.S193793

Wassing IE, Esashi F (2021) RAD51: Beyond the break. *Semin Cell Dev Biol* **113**: 38–46. https://doi.org/10.1016/j.semcdb.2020.08.010

Weivoda MM, Youssef SJ, Oursler MJ (2017) Sclerostin expression and functions beyond the osteocyte. *Bone* **96**: 45–50. https://doi.org/10.1016/j.bone.2016.11.024

Xian L, Wu X, Pang L, Lou M, Rosen CJ, Qiu T, Crane J, Frassica F, Zhang L, Rodriguez JP, Jia X, Yakar S, Xuan S, Efstratiadis A, Wan M, Cao X (2012) Matrix IGF-1 maintains bone mass by activation of mTOR in mesenchymal stem cells. *Nat Med* **18**: 1095–10101. https://doi.org/10.1038/nm.2793

Xue Y, Tong L, LiuAnwei Liu F, Liu A, Zeng S, Xiong Q, Yang Z, He X, Sun Y, Xu C (2019) Tumorinfiltrating M2 macrophages driven by specific genomic alterations are associated with prognosis in bladder cancer. *Oncol Rep* **42**: 581–594. https://doi.org/10.3892/or.2019.7196

Yan J, Herzog JW, Tsang K, Brennan CA, Bower MA, Garrett WS, Sartor BR, Aliprantis AO, Charles JF (2016) Gut microbiota induce IGF-1 and promote bone formation and growth. *Proc Natl Acad Sci U S A* **113**: E7554–E7563. https://doi.org/10.1073/pnas.1607235113

Yang JX, Xie P, Li YS, Wen T, Yang XC (2020) Osteoclast-derived miR-23a-5p-containing exosomes inhibit osteogenic differentiation by regulating Runx2. *Cell Signal* **70**: 109504. https://doi.org/10.1016/j.cellsig.2019.109504

Yin N, Zhu L, Ding L, Yuan J, Du L, Pan M, Xue F, Xiao H (2019) MiR-135-5p promotes osteoblast differentiation by targeting HIF1AN in MC3T3-E1 cells. *Cell Mol Biol Lett* **24**: 51. https://doi.org/10.1186/s11658-019-0177-6

Yoshida T, Delafontaine P (2020) Mechanisms of IGF-1-mediated regulation of skeletal muscle hypertrophy and atrophy. *Cells-Basel* **9**: 1970. https://doi.org/10.3390/cells9091970

Zhang X, Ma N, Yao W, Li S, Ren Z (2019) RAD51 is a potential marker for prognosis and regulates cell proliferation in pancreatic cancer. *Cancer Cell Int* **19**: 356. https://doi.org/10.1186/s12935-019-1077-6

Zhao SJ, Kong FQ, Jie J, Li Q, Liu H, Xu AD, Yang YQ, Jiang B, Wang DD, Zhou ZQ, Tang PY, Chen J, Wang Q, Zhou Z, Chen Q, Yin GY, Zhang HW, Fan J (2020) Macrophage MSR1 promotes BMSC osteogenic differentiation and M2-like polarization by activating PI3K/AKT/GSK3beta/beta-catenin pathway. *Theranostics* **10**: 17–35. https://doi.org/10.7150/thno.36930

Zuo R, Liu M, Wang Y, Li J, Wang W, Wu J, Sun C, Li B, Wang Z, Lan W, Zhang C, Shi C, Zhou Y (2019) BM-MSC-derived exosomes alleviate radiation-induced bone loss by restoring the function of recipient BM-MSCs and activating Wnt/beta-catenin signaling. *Stem Cell Res Ther* **10**: 30. https://doi.org/10.1186/s13287-018-1121-9